

# Right ventricular three-dimensional architecture, assessed with DTMRI, is preserved during experimentally induced right ventricular hypertrophy

E. A. Nielsen<sup>1</sup>, M. Smerup<sup>1</sup>, P. Agger<sup>1</sup>, J. Frandsen<sup>2</sup>, M. Pedersen<sup>3</sup>, S. Ringgaard<sup>3</sup>, P. Vestergaard<sup>2</sup>, J. R. Nyengaard<sup>4</sup>, J. B. Andersen<sup>4</sup>, P. P. Lunkenheimer<sup>5</sup>, R. H. Anderson<sup>6</sup>, and V. Hjortdal<sup>1</sup>

<sup>1</sup>Department of Cardiothoracic & Vascular Surgery, Aarhus University Hospital, Skejby, Aarhus, Denmark, <sup>2</sup>Center for Functionally Integrative Neuroscience, Aarhus University Hospital, Aarhus Sygehus, Aarhus, Denmark, <sup>3</sup>MR Research Center, Aarhus University Hospital, Skejby, Aarhus, Denmark, <sup>4</sup>Stereology and EM Laboratory and MIND Center, Aarhus University, Aarhus, Denmark, <sup>5</sup>Klinik und Poliklinik für Thorax-, Herz- und Gefäßchirurgie, University Münster, Münster, Germany, <sup>6</sup>Cardiac Unit, Institute of Child Health, University College, London, United Kingdom

## Introduction

The three-dimensional architecture of the myocytes making up the right ventricular myocardium is a major determinant of function, but as yet no investigator-independent methods have been used to characterize either the normal or hypertrophied state. Our aim was to assess and compare, using diffusion tensor MRI (DTMRI), the normal architecture with the arrangement induced by chronic hypertrophy.

## Materials and methods

We randomized 20 female piglets, each weighing 5 kg, into 2 groups. In one group, the pulmonary trunk was banded, and in another we performed sham operations. We assessed the extent of right ventricular hypertrophy after 8 weeks using a Philips Achieva 1.5 T MRI system. A stack of 12 cine short axis slices was acquired, covering the left and right ventricles. After sacrificing the pig, the heart was excised and examined with DTMRI to determine the helical angles of the myocytes aggregated within the walls, and the presence of any reproducible tracks formed by the aggregated myocytes. The hearts were allowed to adjust to room temperature, and placed in the scanner with the long axis of the left ventricle aligned parallel to the axis of the main magnetic field. Scout imaging was used to precisely adjust the axis and rotation of the images relative to the heart. Diffusion tensor MRI measurement was performed using a standard multi-slice spin echo sequence with diffusion gradients. The following imaging parameters were used: scan time 12 – 16 h per heart, depending on size, 32 isotropically distributed diffusion directions with the b-factor equal to 1270 s/mm<sup>2</sup> and one with b=0 s/mm<sup>2</sup>, 46-54 slices with 1.33 mm slice thickness and no gap, field-of-view 170x100 mm<sup>2</sup> and a voxel size of 1.33x1.33x1.33 mm<sup>3</sup>. Using custom-made software, we calculated the primary diffusion eigenvector in each voxel, normalizing the value at each voxel according to the values of the matrix as a whole to achieve comparability between different hearts. Helix angles were defined as the projected angle of myocytes onto the tangential plane of the epicardium in any myocardial region measured relative to the transverse plane of the left ventricle. In the present study the angle is reported as a function of myocardial depth in percent, with the epicardial border set to 100%. We measured helix angles in a few selected voxels at predetermined locations at the right ventricle.

## Results

All animals undergoing banding had developed significant right ventricular hypertrophy, albeit no difference was observed in terms of helical angles or myocardial pathways between the banded animals and those undergone the sham operation. The trackings or pathways which pass through the chosen voxel of interest were calculated by the algorithm using the characteristics of the primary eigenvector of all voxels in the total matrix. The paths were color-coded to clearly visualize up to eight structurally different pathways. Voxels were selected at a few predetermined locations, specifically in the outlet of the RV (RVOT), the basal and the apical lateral free wall of the RV, the septum (apical and basis) and the pulmonary/aortic-septum. Helical angles varied from approximately 70° endocardially to -50° epicardially, see figure 2. Very few tracks were circular, with helical angles approximating zero. Reproducible patterns of chains of aggregated myocytes were observed in all hearts see figure 1.

## Discussion

The architecture of the myocytes aggregated together to form the walls of the right ventricle is comparable to that found in the left ventricle in terms of endocardial and epicardial angulations of the chains of aggregated myocytes, albeit that the right ventricle lacks the extensive zone of myocytes aggregated in circular fashion in the mid-portion of the left ventricular walls. These circular tracks were not observed in the right ventricular walls even in the hearts from the banded pigs. Without such beneficial architectural remodeling, the porcine right ventricle seems unsuited structurally to sustain a permanent increase in afterload. Recent reports (1), however, have documented angles of intrusion which is not addressed in this study, though we speculate that this may reflect an inherent flaw in the technique of diffusion tensor magnetic resonance imaging. The chosen voxels of interest measure approximately 1 mm<sup>3</sup>, whilst the average myocyte measures approximately 20x20x100 μm<sup>3</sup>. The primary eigenvector, therefore, represents the mean direction in the chosen voxel of at least 25.000 myocytes, some of which may diverge at significantly greater angles relative to the tangential plane of the cavities.

## References:

1: Lunkenheimer PP, Redmann K, Florek J, Fassnacht U, Cryer CW, Wubbeling F, Niederer P, Anderson RH. 2004. The forces generated within the musculature of the left ventricular wall. Heart 90:200-207.

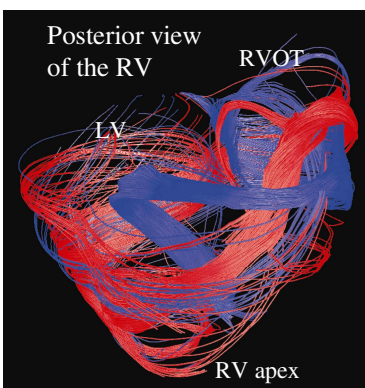
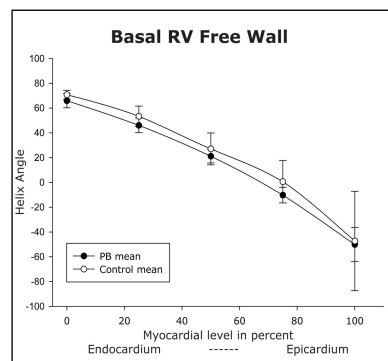


Figure 1. DTMRI of the heart  
Proc. Intl. Soc. Mag. Reson. Med. 17 (2009)



3772

Figure 2, helix angles of the RV free wall